Lithuanian Journal of Physics, Vol. **44**, No. 6, pp. 465–476 (2004)

FORMATION AND INVESTIGATION OF POROUS SiO_2 FILMS ON Si *

R. Šustavičiūtė [a,b], I. Šimkienė [a,b], J. Sabataitytė [a], A. Rėza [a], A. Kindurys [a], R. Tamaševičius [a,c], and J. Babonas [a,c]

[a] *Semiconductor Physics Institute, A. Goštauto 11, LT-01108 Vilnius, Lithuania*
[b] *Vilnius University, Saulėtekio 9, LT-10222 Vilnius, Lithuania*
[c] *Vilnius Gediminas Technical University, Saulėtekio 11, LT-10223 Vilnius, Lithuania*

Received 1October 2004

Porous silica layers on Si substrates were produced by sol–gel spin-on technique. The structural studies and ellipsometric measurements have been carried out in order to investigate the dependence of silica properties on growth technology and thermal annealing. The dense SiO_2 layers from acid tetraethoxysilane-based precursors and the layers of increased porosity obtained from precursors containing surfactant cethyltrimethylammonia bromide were investigated. The hybrid type Fe-doped silica layers were also produced and studied. The provided investigations have shown that the method used is perspective for fabrication of porous silica layers and for obtaining hybrid samples.

Keywords: silica layers, morphology, ellipsometry

PACS: 61.43.–j, 61.43.Gt, 78.66.Nk, 78.66.Sq

1. Introduction

Porous materials have wide potential applications in science and industry [1]. In particular, hybrid nanostructures with special optical and magnetic properties can be produced by filling nanosized pores in a dielectric media with metal, semiconductor materials or organic molecules [2]. For this reason, formation of porous films by a simple sol–gel technique is widely studied [3]. The most attractive feature of sol–gel technology is a possibility to form thin films of different physical properties by mixing sol with the solutions of various compositions. As a porous medium, SiO_2 is most frequently used due to its thermal stability, mechanical resistance, and hydrophily.

In this work porous SiO_2 films on Si substrates were investigated. The samples were fabricated by sol–gel spin-on technique. Sol–gel technology is a perspective inexpensive method for a formation of porous silica films at room temperature. This method allows one to vary the structural and physical properties of silica in a wide range. Tetraethoxysilane (TEOS)-based colloid acid solutions were used as precursors. The porosity of silica films was controlled by various growth and thermal procedures and by introducing a surfactant cethyltrimethylammonia bromide (CTAB) as a template into the precursor.

The morphology and optical properties of the samples were studied by scanning electron microscopy (SEM), atomic force microscopy (AFM), and ellipsometry. The silica films were characterized by morphology and optical parameters. The dependence of silica characteristics on the composition of the precursor and technology was studied. In Section 2, the experimental techniques used in this work are generally described. The growth method (Section 2.1) and optical measurements (Section 2.2) using null- and spectroscopic ellipsometry are described. The details of technology for each sample groups are given below along with the presentation and discussion of experimental results (Section 3). Three main sample groups have been investigated. Relatively dense silica films on a Si substrate are discussed in Section 3.1. In Section 3.2 the results obtained on silica layers of increased porosity which have been fabricated by using surfactants are presented. In Section 3.3 the hybrid-type samples SiO_2:Fe/Si are discussed. At the end of the paper, the results of experimental studies are summarized.

* This work was reported at the International Conference on Structure and Spectroscopy, September 23–26, 2004, Vilnius, Lithuania.

ISSN 1648-8504

2. Experimental

2.1. Formation of porous silica layers by sol–gel spin-on technique

Thin films of silica with controlled porosity were formed by sol–gel technique and deposited on Si substrates by spin coating method. Porous silica was produced by hydrolysis and condensation of alkosilanes. The alcohol solution of TEOS with small amount of water and acid or base catalyst was used as a precursor. Due to a high speed of the hydrolysis process

$$\mathrm{Si(OC_2H_5)_4 + H_2O} \rightarrow \mathrm{Si(OC_2H_5)_3(OH) + C_2H_5OH}, \quad (1)$$

TEOS is an optimal precursor for silica. Simultaneously with hydrolysis, a polymerization process occurs:

$$\equiv\mathrm{Si{-}OH + \equiv Si{-}OH} \rightarrow \equiv\mathrm{Si{-}O{-}Si\equiv + H_2O}, \quad (2)$$

$$\equiv\mathrm{Si{-}OC_2H_5 + \equiv Si{-}OH} \rightarrow \equiv\mathrm{Si{-}O{-}Si\equiv + C_2H_5OH}. \quad (3)$$

During the latter reactions, the sol is formed. At condensation, two hydrolysed fragments join together and either water (2) or alcohol molecules (3) are released. The condensation occurs by nucleophilic substitution or addition, i. e. when monomers join into polymers during a condensation reaction. A complete hydrolysis-condensation reaction is described by the following equation:

$$n\mathrm{Si(OC_2H_5)_4} + 2n\mathrm{H_2O} \rightarrow n\mathrm{SiO_2} + 4n\mathrm{C_2H_5OH}. \quad (4)$$

In this way, the main polymeric chains, which consist of Si atoms joint together by oxygen, are formed.

Thus, the polymerization runs in three stages [4]: (i) formation of monomers; (ii) occurrence of polymeric chains in sol; (iii) coagulation of polymeric chains into gel. The acidity of colloidal solution favours hydrolysis. Therefore, under acid conditions the elements can be completely hydrolysed before condensation takes place. Thus, short chains form, and a dense final product [5] is produced after drying. Base environment favours condensation. Therefore, under base conditions the condensation starts before hydrolysis is ended. Rapid polymerization occurs and the particles, which form in a few minutes, quickly grow from 1–2 nm to 100–150 nm until equilibrium settles [6]. As a result, silica layers formed by sol–gel technique from base solutions possess large particles [4] and are not stable in time [7].

Thus, the shape of the polymers $(\mathrm{SiO_2})_n$ depends on the technological parameters as the type and concentration of precursor and solvent, catalyst, water concentration, pH value of solution, temperature, and gelling time. Polymers, the stability of which chemical bonds ascertain, present chains, bands, and frames.

The solution is poured into a vessel and dried. As seen from Eqs. (2) and (3), at condensation small water and alcohol molecules are released and evaporate under drying. When solvent evaporates, the coordination of particles increases under the influence of surface tension forces, the particles join intensively, and the frame deforms. When the frame becomes strong enough to withstand the surface tension, the voids form. In other words, when gel is drying, the frame, which has been composed in solution, becomes denser and deforms due to formation of voids. Thus, the structure of dried gel, i. e. xerogel, consists of a skeleton frame and voids.

The shape, size, and density of pores depends on formation technology and further post-growth annealing, during which molecular water is excluded and amorphous structure of $\mathrm{SiO_2}$ is formed. In order to control additionally the porosity of the synthesized material, large organic molecules are inserted into silica sol [8, 9]. In silica sol the groups of organic molecules form micelles, which act as a template. Relatively small oligomers of silicates adsorb on the active surface of large-radius surfactant micelles. When gel is dried, organic molecules are excluded chemically or by annealing. As a result, porous matrix of silicon oxide is formed in which the size of pores corresponds to the size and shape of surfactant micelles or their aggregates in sol.

On the one hand, bulk silica gels are widely applied as adsorbents and catalysts. On the other hand, the sol–gel technology is perspective for production of porous silica layers for optoelectronic devices. By choosing the composition of solution, the surface films with controlled optical reflectance, transmission, and absorption can be fabricated.

Using the sol–gel technique, the layers can be formed by dipping the substrate into the solution, spraying the solution on a substrate or by spin-coating using a centrifuge. As compared with dipping technique, the spin coating method has some advantage as by the latter method large-area layers of a uniform thickness are produced. The layers weakly depend on

the type of the substrate. However, the properties of the layers obtained by sol–gel spin-coating differ from those of bulk xerogels. The difference is caused by various conditions of structure formation. Drying and formation of the gel structure go on for weeks and months in xerogels whereas it takes several tens of seconds in the layers produced by spin-coating. The process of the structure formation during spin-coating is not well studied as yet.

By choosing the synthesis parameters such as acidity of solution (pH value), temperature, rotation speed of the centrifuge, and the type of the template, different silica layers were synthesized with varying porosity. The technology in each particular case will be described below at the presentation of experimental results and their discussion.

2.2. Optical measurements

The optical properties of silica films were studied by ellipsometry technique, which is based on the analysis of light polarization [10]. When the light of known polarization is incident, the polarization of the light reflected from the sample is measured. From the analysis of the polarization ellipse, the ratio ρ of the complex amplitude reflection coefficients $R_{\rm p}$ and $R_{\rm s}$ for light polarized parallel (p) and perpendicular (s) to the plane of incidence

$$\rho = \frac{R_{\rm p}}{R_{\rm s}} = \tan\Psi \exp(\mathrm{i}\Delta) \tag{5}$$

is measured and the ellipsometric parameters, i. e. angles Ψ, Δ, are determined. The ρ value is directly related to the complex dielectric function ε of the sample:

$$\varepsilon = \left[\left(\frac{1-\rho}{1+\rho}\right)^2 \tan^2\theta + 1\right] \sin^2\theta, \tag{6}$$

where θ is the angle of the light beam incidence.

In the case of thin films deposited on the substrate [11], the reflections from both film and substrate should be considered. The Fresnel reflection coefficients at the interfaces air–film and film–substrate were calculated taking into account the Snellius law.

For a complex system of a stack of layers on the substrate surface, the optical response of this multilayer structure was analysed by a transfer-matrix technique [12] modelling the propagation of an electromagnetic wave by introduction of a 2D vector for electric and magnetic fields taking into account the boundary conditions at the interface between the layers. Each jth layer was characterized by the matrix

$$M_j = \begin{vmatrix} \cos\beta_j & (\mathrm{i}/\widetilde{N}_j)\sin\beta_j \\ \mathrm{i}\widetilde{N}_j \sin\beta_j & \cos\beta_j \end{vmatrix}, \tag{7}$$

where $\beta_j = (2\pi n_j d_j/\lambda)\cos\theta_j$ is the phase thickness, $\widetilde{N}_j = n_j/\cos\theta_j$ for p-polarization, and $\widetilde{N}_j = n_j\cos\theta_j$ for s-polarization, θ_j being the angle of incidence, $\varepsilon_j = n_j^2$ is the dielectric function, and d_j is the thickness of the jth layer.

In this work both null- and spectroscopic ellipsometry techniques were used. Using the null-ellipsometer LEF-3M, which is operating at 633 nm (He–Ne laser), the dependence of ellipsometric parameters on the angle of light incidence was determined. The experimental data were fitted by the model of a homogeneous layer on the substrate and the averaged values of the dielectric function and thickness for silica layers were calculated. The porosity of the silica layer was evaluated from the obtained value of the refraction index as compared with that for the reference data [13].

A photometric spectroscopic ellipsometer with a rotating analyser was used in the range 0.5–5.0 eV. The detector signal was processed on-line by nonlinear regression analysis. The characteristic ellipsometric angles Ψ, Δ were measured with an accuracy of 0.02°. The details of the experimental set-up are presented elsewhere [5]. The experimental data were described by the model calculations with adjustable parameters like dielectric function, thickness, and porosity of the layers.

2.3. Structural studies

The morphology and structure of silica layers were studied by the standard SEM and AFM techniques. The atomic force microscope Explorer was used in the contact mode and the images of area from 1×1 μm^2 to 100×100 μm^2 were obtained with a resolution of 300×300 pixels. A scanning electron microscope SUPRA 35 with resolution from 2.5 nm at 1 kV to 1.7 nm at 15 kV was used and the micrographs were obtained with 3072×2304 pixels.

3. Results and discussion

3.1. Dense silica layers

As noted above, silica layers can be produced by several methods. In this work the dense SiO_2 films

on the Si substrate obtained by thermal annealing were used for control measurements.

3.1.1. Thermally oxidized Si wafers

Thermal oxidation of Si wafers is a technique which is most widely applied for production of dense silica films in electronic devices. The (111)-oriented n-Si wafers of resistance 1 Ω·cm were annealed at 1150 °C in dry oxygen for time varying in the range of 5–20 min.

Figure 1 shows the spectral dependence of ellipsometric parameters for the Si surface thermally oxidized for 15 min. The experimental data were described by the system SiO_2/Si taking into account a possible non-homogeneity of the silica layer by dividing the film into 6 sublayers. The reference data for the dielectric function of Si [14] and SiO_2 [13] were used. In the fitting procedure the thickness and porosity of each silica sublayer were considered as adjustable parameters. From the values of optimal fitting (Fig. 1) for this particular case, the thickness of each 6 sublayers was in the range of 20–25 nm with the total thickness of the silica layer 134 nm. The porosity of sublayers varied in the range of 50% and decreased from the surface towards substrate. For a series of the thermally oxidized Si wafers it was found that the thickness of the silica layer depended linearly on the annealing time.

A perfect correspondence between experimental and simulated data confirmed the validity of the accepted approach. It should be noted that a worse agreement was obtained for a simple model of a uniform silica layer.

3.1.2. Layers processed by sol–gel technique

Preparation. For preparation of dense though porous layers of SiO_2 by sol–gel technique, liquid compositions of $Si(OC_2H_5)_4$–C_2H_5OH–H_2O–HCl at the volume ratio $20:40:4:0.1$ were used. The main oxide component TEOS $Si(OC_2H_5)_4$ was dissolved in alcohol with addition of catalyst HCl and a small amount of H_2O for a hydrolysis of TEOS. The acid solution with pH ≈ 2 favours rapid hydrolysis, and the sol forms in it in 24 h. Sol of this acidity is stable. The formed colloid particles of 2–4 nm in size stop to enlarge because of the equilibrium between polymerization and depolimerization and join into linear aggregates [4].

The sol is deposited in 30–60 s on (100)-oriented n-Si (0.5 Ω·cm) wafers mounted in a centrifuge rotating at a speed of 1000–2500 rpm. The solvent evaporates during rotation and a film forms the thickness of which depends on the rotation speed of the centrifuge.

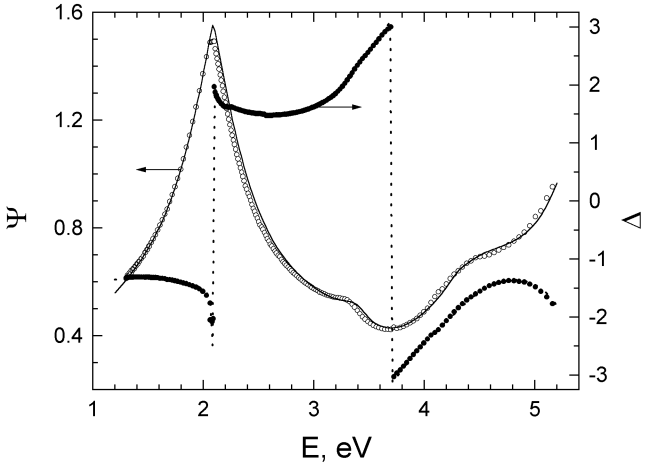

Fig. 1. Experimental (points) and calculated (curves) spectra of ellipsometric parameters for the SiO_2 layer formed by thermal annealing (15 min at 1150 °C in dry oxygen) on n-Si.

At the next step the layers are dried at 80–100 °C for 1 h and annealed in air or argon at 300–700 °C for 1–2 h. As a result, the layers of thickness 0.1–0.2 μm are obtained on the substrate surface.

Morphology. Observations under an optical microscope have shown that dense silica layers produced by sol–gel spin-on technique are quite smooth and homogeneous. The morphology of annealed samples was studied by the AFM technique. In Fig. 2 the AFM pattern is presented for the SiO_2 layer, which has been processed from acid solution, dried at 80 °C, and then annealed for 1 h at 300 °C in air and for 2 h at 550 °C in argon. As seen from Fig. 2(a), the surface is dense and smooth though some inclusions of 1 μm in height are observed. The fine structure of the surface (Fig. 2(b)) shows the roughness of the surface of the order of 250 nm. The rectangular-shaped particles of size $\sim 50 \times 50$ nm^2 and $\sim$50 nm in height are crystallized on the rough surface. The regularly-shaped nano-sized particles are characteristic of silica layers produced by the sol–gel spin-on technique and annealed in Ar, in contrast to amorphous silica layers obtained by dip coating and annealed in air [15].

Optics. The studies of the samples by null-ellipsometry have shown that silica layers produced by the sol–gel spin-on technique on Si substrates were quite dense and homogeneous. The porosity of SiO_2 layers dried at 103 °C for 1 h was 9% at the centre of the Si wafer with ∅5 cm and 5% at the edge of the wafer.

The annealing of the samples has led to an increase of refraction index for SiO_2, hence to a decrease of porosity. Figure 3 shows the results of the null-ellipsometry measurements and the dependence of the

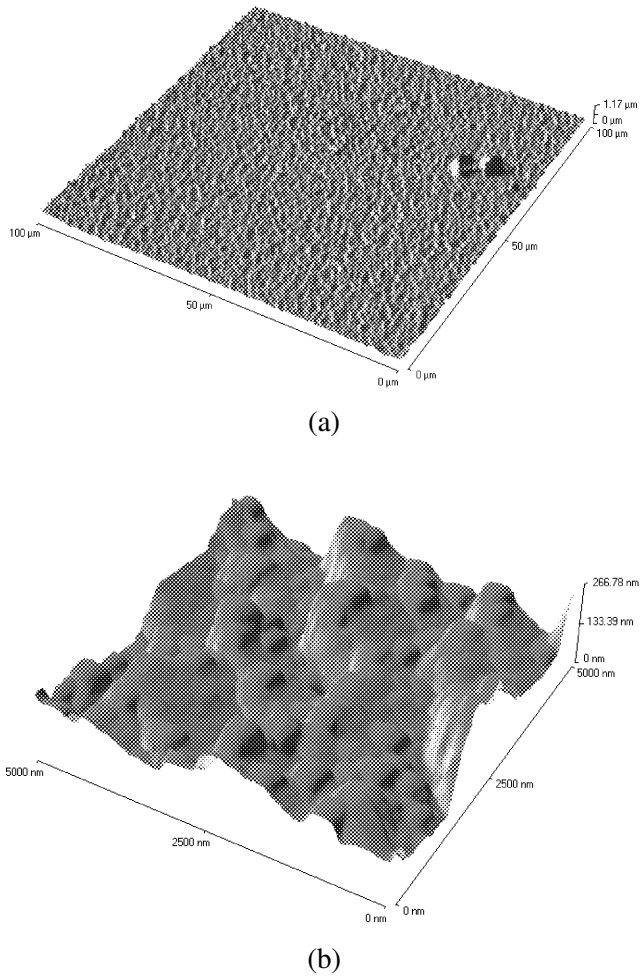

Fig. 2. AFM surface images of the area (a) 100×100 μm^2 and (b) 5×5 μm^2 of the sol–gel processed and annealed (in air 1 h at 300 °C and in argon for 2 h at 550 °C) SiO_2/Si sample.

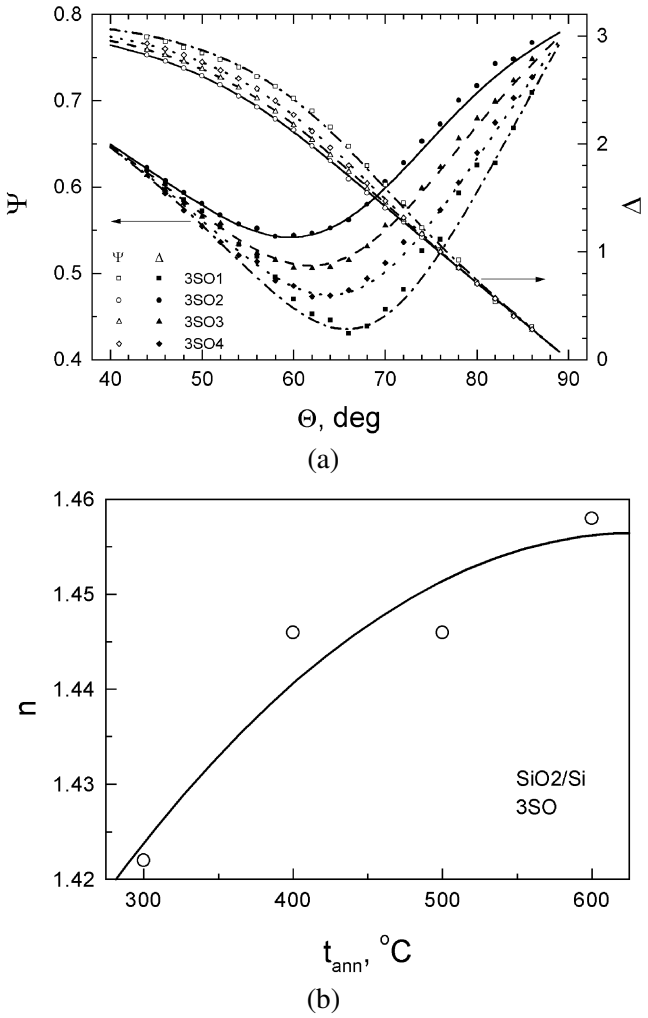

Fig. 3. Null-ellipsometry data for dense sol–gel processed SiO_2 films on Si annealed at various temperatures $t_{\rm ann}$ in the range 300–600 °C. (a) Experimental (points) and calculated (curves) angular dependence of ellipsometric parameters. (b) The dependence of the refraction index of silica films on the annealing temperature obtained from the data presented in (a). The curve in (b) is a guide for an eye.

refraction index of the silica layers at the annealing temperature $t_{\rm ann}$. As seen from Fig. 3(a), experimental data are quite well described by the simple one-layer model. Figure 3(b) shows that the refraction index of the SiO_2 layer is increasing with an increase of $t_{\rm ann}$.

The obtained results are in a good agreement with the data obtained on silica layers produced by sol–gel technique from TEOS and aqueous ammonia solution in ethanol [16]. In [16] it was found that refraction index of these silica layers increased from 1.430 to 1.450 for samples dried at 60 °C and annealed at temperatures of up to 800 °C. It is interesting to note that the refraction index of the sol–gel silica films was smaller than of those fabricated by dipping technique. In the latter case, the refraction index varied in the range of 1.445–1.457 for the samples annealed under similar conditions.

Some discrepancy between experimental results and the data calculated in a one-layer model can be due to some in-depth nonhomogeneity of SiO_2 films. The experimental results obtained by spectroscopic ellipsometry and modelling have shown that a better agreement was achieved considering the silica layer as a stack of multilayers. Figure 4 presents the results for the SiO_2 film of total thickness 245 nm which has been dried at 103 °C for 5 min and the simulation data for a stack of 5 silica layers with different porosity varying in the range of 7–23%. As a whole a good agreement between experimental and calculated data was achieved. Some discrepancy in the high-energy region can be due to a short drying time at low temperature.

Some in-depth nonhomogeneity of sol–gel spin-on processed silica layers was also confirmed by variable angle spectroscopic ellipsometry measurements. The

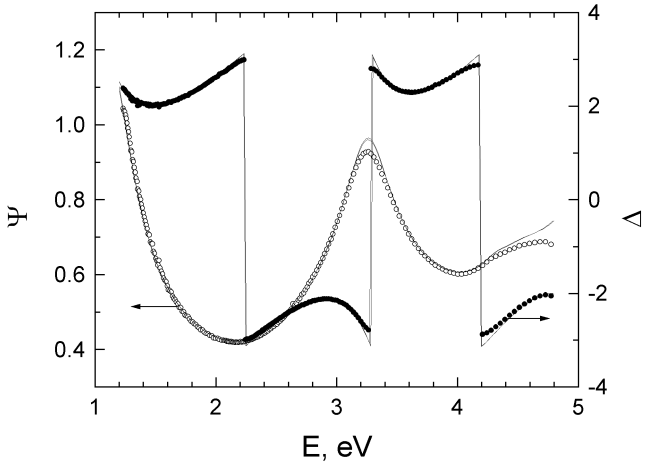

Fig. 4. Experimental (points) and calculated (curve) spectral dependence of ellipsometric parameters for the sol–gel processed SiO_2 layer on the Si substrate dried at 103 °C for 5 min.

best agreement between the experimental data and the model calculations was obtained at slightly (5–7%) different values of adjustable parameters, when the results of ellipsometric measurements at various angles of light incidence were treated separately. However, an increase of the number of sublayers did not lead to the fitting improvement indicating that nonhomogeneity of dense sol–gel spin-on processed SiO_2 layers is mainly due to inclusions and possibly to the presence of suboxides and remnants of chemical reactions.

Perspectives for application. The studies provided have shown that the SiO_2 layers formed by the sol–gel spin-coating technique from acid TEOS colloidal solution and annealed in air/argon are dense, homogeneous, and are characterized by a small porosity. These silica layers are suitable for surface passivation and formation of masking coatings in the technological processes of semiconductor electronic and optoelectronic devices. However, the porosity of these silica layers is too small for production of hybrid structures consisting of nanoparticles of metals and their oxides in dielectric media.

3.2. Layers of increased porosity

As noted above (Section 2.1), the porosity of bulk xerogels can be varied by introducing organic molecules into the precursor. In solutions organic molecules coagulate into nanometric-sized aggregates, surfactant micelles, possessing an active surface which attracts Si–O molecules. After drying the xerogel and excluding organic molecules, porous bulk silica is obtained with pores, the size of which correspond to that of micelles or their aggregates.

The properties of silica layers prepared by sol–gel spin-on technique from base solutions with surfactant were studied in [7]. It was found that the silica layers were not stable. The porosity evaluated from refractive index and the stretching frequency due to –OH group of chemisorbed hydrated ammonia varied in time for 20 days.

The role of surfactant on the formation of sol–gel processed silica layers from acid solutions was not investigated as yet. For this reason, in this work we have prepared the silica layers from precursors with surfactant CTAB and studied their morphology and physical properties.

Preparation. The colloid solution was prepared by mixing TEOS and ethanol in ratio 5.1 and 8.1 ml, respectively. Water solution of concentrated hydrochloric acid in amount of 3 ml was added into colloid solution and mixed in a sonic bath for 15 min. Two solutions of surfactant in amount of 10 ml each were prepared by dissolving 0.34 g of CTAB in ethanol (I) and water (II) and mixing in an ultrasonic bath. The TEOS-based colloidal solution in amount of 5.4 ml was mixed with 10 ml of surfactant solution I (or II) and shaked ultrasonically for 2 h to intensify hydrolysis of TEOS. The final precursor solutions with surfactant solutions I and II were characterized by molar compositions

$$1\,\mathrm{TEOS} + 22\,\mathrm{C_2H_5OH} + 5\,\mathrm{H_2O} + 0.004\,\mathrm{HCl} + 0.096\,\mathrm{CTAB}$$

and

$$1\,\mathrm{TEOS} + 5\,\mathrm{C_2H_5OH} + 60\,\mathrm{H_2O} + 0.004\,\mathrm{HCl} + 0.096\,\mathrm{CTAB}$$

with acidity pH equal to 2.20 and 1.86, respectively.

Silica layers were deposited in 1 min on n-Si wafers (0.5 Ω·cm, (100)-orientation) placed on a centrifuge rotating at 1000–2000 rpm. The SiO_2/Si samples were dried at ∼150 °C for 5 h, heated slowly up to 500 °C and annealed at this temperature for 1 h.

Morphology. The morphology of these porous silica layers was studied by SEM. As seen from SEM images (Fig. 5), the annealed silica layers are quite dense and smooth. The roughness of the surface did not exceed 20 nm, in contrast to the case of dense SiO_2 layers (Fig. 2), which consisted partially of recrystallized particles. However, large defects of size ∼1 μm are observed which can be related to the remnants of reaction products. In particular, the large (up to 1.5 μm in length) rod-like and spherical particles of ∅50–100 nm

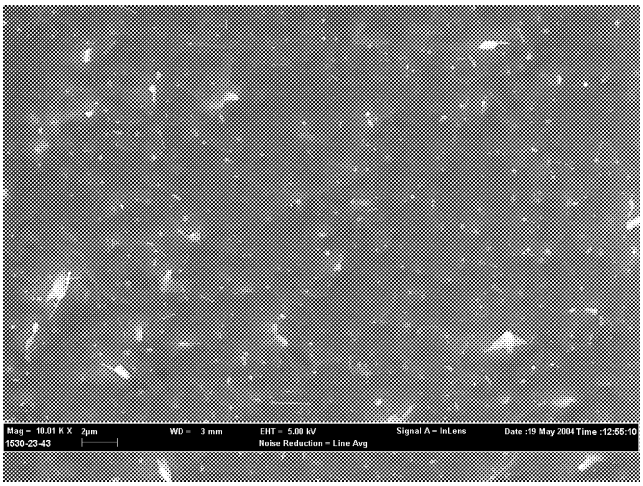

(a)

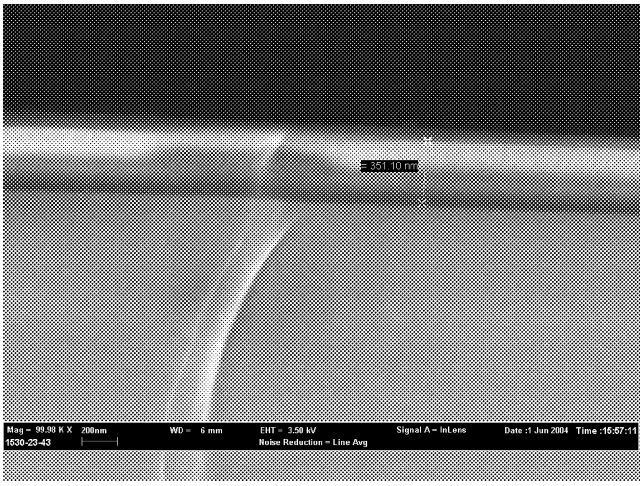

(b)

Fig. 5. SEM micrographs of (a) surface and (b) cross-section of the SiO_2/Si sample produced from precursor with CTAB dissolved in H_2O, dried at 150 °C for 5 h and annealed at 550 °C for 1 h.

are typical of CTAB molecules [9]. The cross-sectional view of the SiO_2/Si sample indicates that the thickness of the silica layer is uniform though the adhesion is quite weak. Note that the defect in the substrate (Fig. 5(b)) influenced the structure of the silica layer.

The structural studies have shown that during spin-coating the surfactant micelles are not destroyed. Therefore, it is reasonable to predict that at reduced concentrations of surfactant it is possible to form spherical CTAB aggregates in SiO_2 layers and hence to obtain regularly distributed nanometric pores.

Optical studies. The null-ellipsometry studies were carried out in order to determine the dependence of porous silica layers on parameters of growth technology. It was found that the refraction index of as-grown silica layers produced from CTAB dissolved in ethanol is equal to ∼1.47 at centrifuge rotation speed

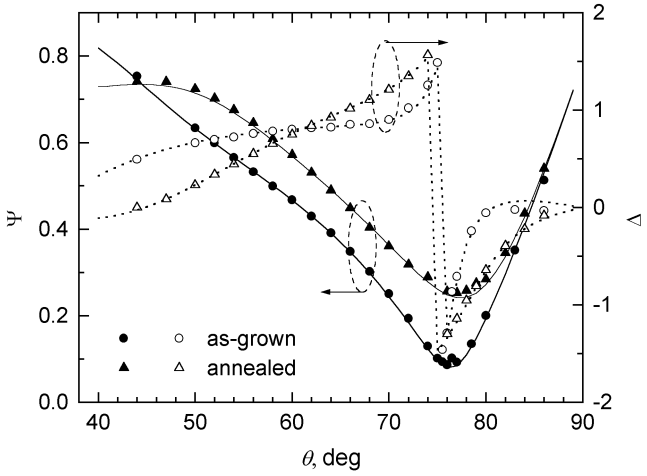

Fig. 6. Experimental (points) and calculated (curves) dependence of ellipsometric parameters Ψ, Δ on the angle of light incidence θ for as-grown and annealed SiO_2/Si samples produced from precursor with CTAB dissolved in ethanol.

of 1000 rpm. Thus, the porosity of as-grown SiO_2 layers was quite small (∼7–10%) as the voids in the silica matrix were filled by organic molecules. Annealing of SiO_2/Si samples has led to an increase of porosity of the silica layer and to a significant decrease in thickness (Fig. 6). This observation clearly demonstrates that during annealing the major part of CTAB is evaporated resulting in formation of porous (∼65%) SiO_2 layers. For the SiO_2/Si sample characterized in Fig. 6, the thickness and dielectric function were 580 nm and 2.156 for as-grown silica layer and 485 nm and 1.451 for the annealed one.

Null-ellipsometry studies have also shown that the refraction index and hence the porosity of SiO_2 layers depend on the solvent in which surfactant CTAB was dissolved. The refraction index of annealed samples was equal to ∼1.20 and ∼1.49 for the silica layers produced from the precursor with CTAB dissolved in ethanol and water, respectively. It is reasonable to assume that this difference is due to the fact that CTAB is better dissolved in ethanol than in water, and therefore, these silica layers are of larger porosity.

An increase of the centrifuge rotation speed results in formation of thinner and denser SiO_2 layers. For example, the refraction index and thickness of silica layers produced from CTAB dissolved in ethanol and annealed in air were ∼1.20, 485 nm and ∼1.23, 325 nm at the centrifuge rotation speed equal to 1000 and 2000 rpm, respectively. Analogous values for SiO_2 layers formed from precursor containing CTAB dissolved in H_2O were ∼1.50, 505 nm and 1.51, 305 nm, respectively, for the same rotation speeds.

3.3. Hybrid samples SiO_2:Fe/Si

As noted above, the advantage of the sol–gel technique is the possibility to form hybrid samples like thin silica layers with metal/metal oxide nanoclusters by mixing the silicate sol with salts of various metals. Using further thermal treatment it is possible to control the microstructure and the chemical composition of the multicomponent silica layer. As a result of such a sol–gel spin-on procedure, in this work the hybrid samples were obtained which consisted of Fe/Fe-oxides nanoclusters imbedded into inert, inorganic, optically transparent, stable, and porous silicon oxide matrix.

It is known [17] that Fe compounds accumulate in the pores of bulk xerogels. In addition, from a mixture of $FeCl_3$ and water solution of CTAB, the nanoparticles of α-Fe_2O_3 are formed [18]. Therefore, it was reasonable to expect that a silica layer with inclusions of Fe oxides could be formed by mixing TEOS sol with CTAB and Fe salts.

Preparation of hybrid samples. In 40 ml of water, an amount of 0.84 g $FeCl_3{\cdot}6H_2O$ and 0.6 g CTAB was dissolved. The solution was ultrasonically shaken to assure a complete dissolution of salts. A drop of the prepared solution was spread over the surface of a Si wafer (n-type, (100)-plane, 0.5 $\Omega{\cdot}$cm). The layer was formed in 1 min in the centrifuge rotating at a speed of 2500 rpm.

The other type of samples was obtained from a precursor of another composition. The in-advance prepared sol of composition $Si(C_2H_5O)_4$ (20 ml) + C_2H_5OH (40 ml) + H_2O (4 ml) + HCl (0.1 ml) was mixed in the volume ratio $1:1$ with another solution of $FeCl_3$ and water solution of CTAB (in the volume ratio $1:1$). The layer was formed on a Si substrate in 1 min in the centrifuge rotating at 2500 rpm. The as-formed layers were dried in air at 80 °C for 4 h and annealed in air for 1 h at 550 °C.

Morphology. Structural investigations by the SEM technique have shown that the surface of as-grown silica layer doped with Fe/Fe–O was quite nonuniform as if it was originated from a very viscous liquid. Large inclusions of size up to 2 μm were noticed. Such a surface is expected to be formed from $FeCl_3$ and water solution of CTAB in silicate sol. It is known [1] that water solution of $FeCl_3$ is a micelle-type colloid, which forms due to a rapid hydrolysis reaction of $FeCl_3$:

$$FeCl_3 + 3H_2O = Fe(OH)_3 \downarrow + 3HCl. \qquad (8)$$

A large number of active $Fe(OH)_3$ molecules occurs. These molecules join together as $(Fe(OH)_3)_m$ forming the cores of colloidal particles. The core surface possesses a base type and attracts the Fe^{3+} ions, which keep electrically chlorine ions around. Hence, the micelles $\{[Fe(OH)_3]_m,\ nFe^{3+},\ 3(n-x)Cl^-\}^{3x+}3xCl^-$ are formed. A rapid process can be stopped by introducing a surfactant into the solution [18]. However, at the interaction of active surfactant micelles, iron hydroxide, and CTAB, the mesa-structure of the silicate layer deforms and favourable conditions for the formation of inclusions occur [19]. The surface structure depends significantly on the interaction at the interface boundaries. Variation of the interactions at the interfaces leads to occurrence of nonhomogeneities at the layer surface.

Figures 7(a, b) present the cross-sectional views of the dried and annealed Fe-doped silica layer formed from precursor containing TEOS and CTAB. As seen, for the as-grown and just dried sample (Fig. 7(a)) the surface roughness is of the order of 50 nm. Small textured particles join together and form smoothly-edged larger roughness of $\sim$100 nm in height and $\sim$1 μm in size. The surface layer of the annealed sample (Fig. 7(b)) is smoother, though some sphere-like particles of $\sim$100 nm are formed.

On the surface of the as-grown and dried sample (Fig. 7(c)) large-sized ($\sim$1 μm) inclusions are noticed. It was proposed [20] that aggregates of surfactant and silicon oxide are formed which surround the core consisting of surfactant micelles. Between these large-sized defects, the pores of $\varnothing$30–100 nm are clearly resolved. The annealed surface is more homogeneous, though the density of pores is increased. It should be noted that the size of pores remains approximately the same as in the as-grown and dried sample. The traces of surfactant disappeared though large inclusions of secondary phases of 500–800 nm are still clearly seen. It is reasonable to assume that Fe–O particles are accumulated at the defects as it was in Fe-doped dense silica layers [21].

Optics. A specific feature of silica layers doped by Fe and Fe–O is that, in contrast to pure silica layers, effective dielectric function ε_{eff} evaluated from null-ellipsometry data is a complex quantity, i. e. it possesses a nonzero imaginary part. This observation indicates that the absorption due to Fe and/or Fe–O is quite significant at the operating wavelength (633 nm) of the null-ellipsometer. The dielectric function ε_{eff} for the Fe–O layer of thickness $\sim$90 nm which has been produced from a precursor containing CTAB and $FeCl_3$ was equal to $(1.353, 0.168)$. For the as-grown

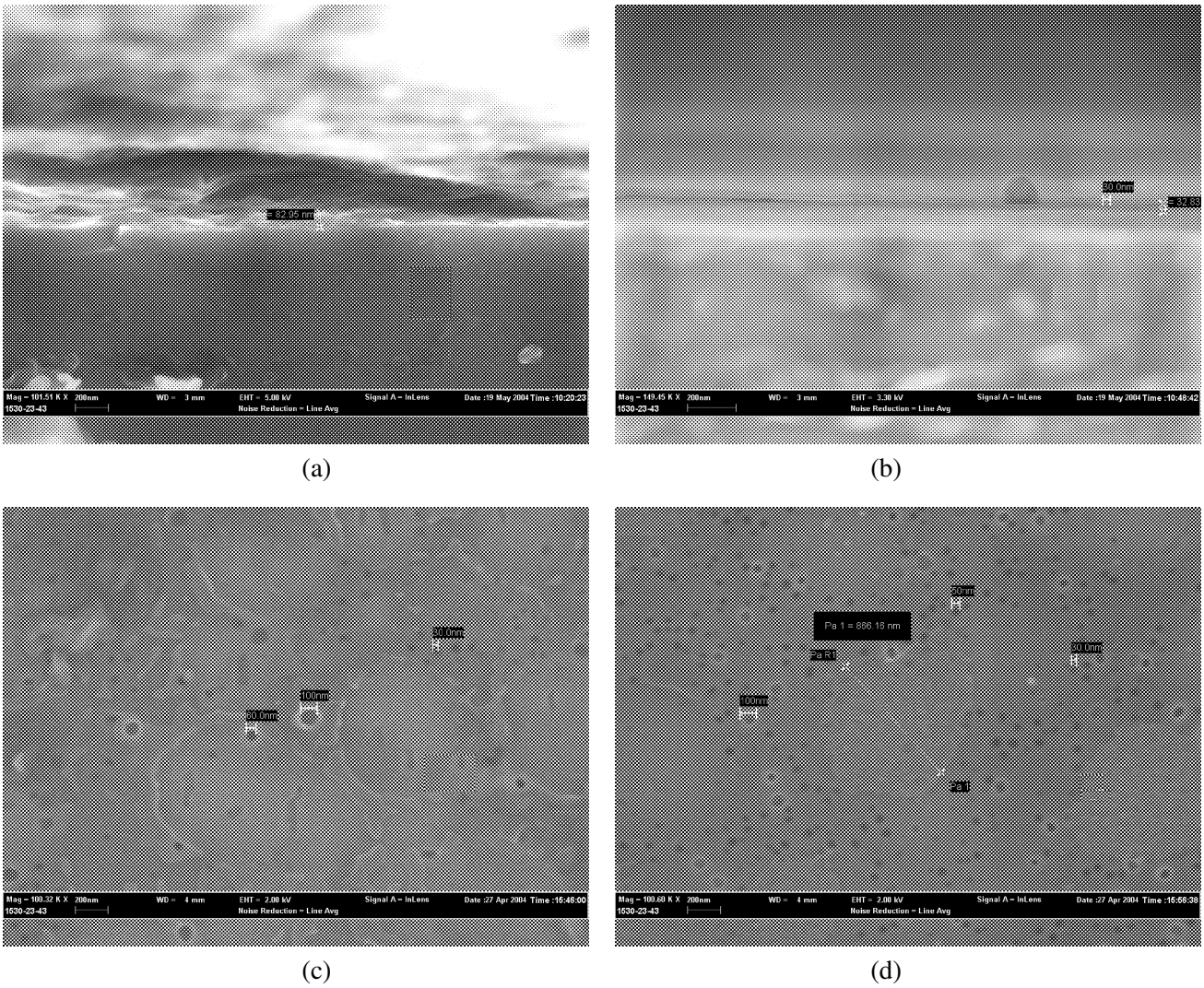

Fig. 7. (a, b) Cross-sectional and (c, d) surface SEM micrographs of dried at 80 °C for 4 h (a, c) and annealed at 550 °C for 1 h (b, d) Fe-doped silica layers formed from the precursor containing TEOS and CTAB.

and annealed Fe-doped silica layer, ε_{eff} is equal to (1.754, 0.252) and (1.946, 0.084), respectively. The latter values show that annealing results in the transformation of Fe oxides.

The optical properties of Fe-doped silica layers were investigated previously for the samples annealed in various atmospheres [21] and for silica layers of different porosity [22]. In this work the spectral dependence of the dielectric function of Fe-doped silica layers will be analysed in more detail.

The other specific feature of Fe-doped porous SiO_2 layers is that, in contrast to the case of dense silica films deposited on Si substrates [21, 22], the interference pattern is not so well resolved in the spectra of ellipsometric parameters (Fig. 8). This is due to a possible nonhomogeneity of the surface layers as well as due to the increased extinction.

In the case of dense Fe-doped silica layers the results of ellipsometric measurements were well described [22] by the combined contributions of effective layers consisting of Fe and Fe oxides. In the case of porous Fe-doped layers this approach was not valid. Therefore, the results of ellipsometric measurements were interpreted by the optical response originating from a stack of three layers each represented by three Lorentzian type lines:

$$\varepsilon(E) = \varepsilon_0 + \sum_j \frac{A_j}{E_j^2 - E^2 - \mathrm{i}E\Gamma_j}, \qquad (9)$$

where A_j, E_j, and Γ_j are oscillator strength, energy, and broadening of the jth Lorentzian line. As seen from Fig. 8, in this approach the calculated results reasonably fit to the experimental data and allow one to

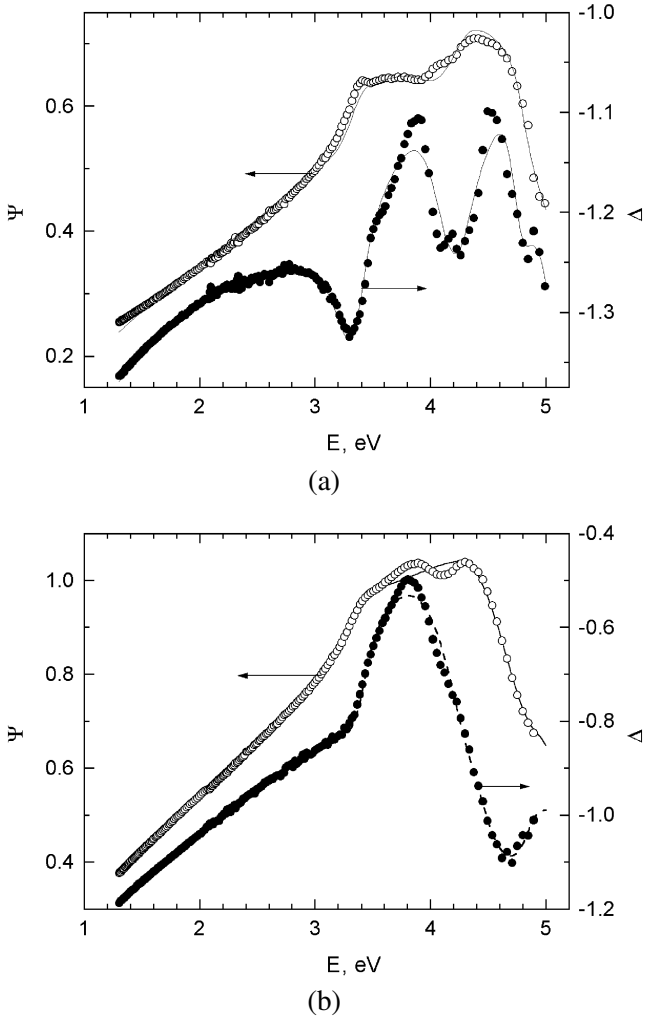

Fig. 8. Experimental (points) and calculated (curves) spectra of ellipsometric parameters Ψ, Δ for the dried (at 80 °C for 4 h) surface layers grown on Si substrates from the precursor containing (a) CTAB + $FeCl_3$ + H_2O and (b) CTAB + $FeCl_3$ + H_2O + TEOS + C_2H_5OH.

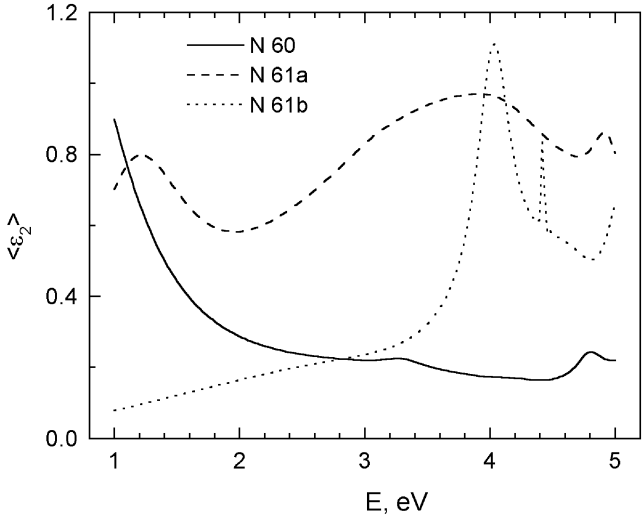

Fig. 9. The effective dielectric function of surface layers on the Si substrate calculated from modelled ellipsometric spectra for dried (at 80 °C for 4 h, samples N 60, N 61a) and annealed (at 550 °C for 1 h, sample N 61b) surface layers grown from the precursor containing CTAB + $FeCl_3$ + H_2O (N 60) and CTAB + $FeCl_3$ + H_2O + TEOS + C_2H_5OH (N 61a, N 61b).

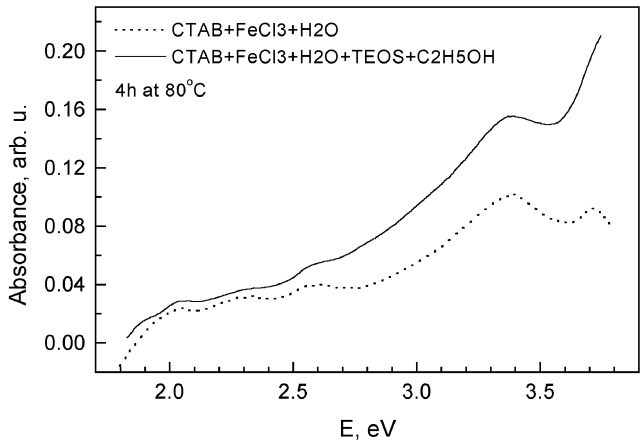

Fig. 10. Absorbance spectra of layers deposited by the spin-coating technique on the glass substrate from precursors denoted in the insert.

analyse particular spectral features characteristic of the surface layers.

The provided analysis has shown that the absorption features typical of the layers of this type (Fig. 9) deposited on Si substrates can be compared with the characteristic features of Fe [23] and Fe oxides [24, 25] with relative intensities varying in particular samples. In the layer produced from CTAB + $FeCl_3$ + H_2O the contributions from the broad band at ∼2.8 eV, absorption rising smoothly towards higher-energy photon region, and infrared absorption band were revealed. These contributions can be related to the optical response of Fe_2O_3 [25], Fe_3O_4 [25], and Fe [23]. Similar contributions can be revealed for the dried and annealed silica layers produced from precursors CTAB + $FeCl_3$ + H_2O + TEOS + C_2H_5OH. However, for the dried layer the contribution due to Fe_2O_3 was strong whereas for the annealed silica layer the higher-energy line was significantly increased. The latter feature can be originated from the particles of Fe_3O_4.

The absorption mechanism due to Fe–O particles in the layers deposited on Si can also be compared with direct absorbance measurements of the similar layers deposited on the glass substrates. As seen from Fig. 10, some weak optical features were observed in the region 2.0–2.7 eV followed by an absorption-edge-like feature with the onset at ∼2.0 eV typical of Fe_2O_3 [24]. The peaks at 3.3 and 3.7 eV in the band of fundamental

absorption can be correspondent to absorption features for Fe_3O_4 [25]. Nevertheless, from the chemical considerations [23] it follows that the dominant Fe compound in this case should be FeOOH.

The analysis of the optical data has shown that a variety of Fe compounds were formed in the Fe-doped porous silica layers produced by the sol–gel spin-on technique. It is reasonable to assume that further annealing in different atmospheres can lead to formation of dominating Fe–O as it was noticed in dense Fe-doped silica layers [21].

4. Summary

The dense uniform silica layers of average porosity 5–9% and roughness ∼250 nm were produced on Si wafers of ∅5 cm by the sol–gel spin-on technique from acid TEOS-based precursor. The porosity varied in depth in the range of 7–23% for silica layers of the total thickness ∼250 nm. The average refraction index of silica layers annealed at the temperatures in the range 300–600 °C was equal to 1.42–1.46 indicating a decrease of porosity. The silica layers of increased porosity were produced from a precursor containing surfactant CTAB. In this series of the samples, the porosity of annealed silica layers was ∼65% as compared with porosity of 7–10% for as-grown samples. In porous silica layers the Fe-containing particles were most presumably in the form of Fe oxides Fe_2O_3, Fe_3O_4, and FeOOH, and the relative amount of Fe_3O_4 was increased in the annealed samples.

Acknowledgements

The authors are thankful to Dr. S. Balakauskas for manufacturing the samples of SiO_2/Si with thermal oxide layers for control measurements and to A. Kalinichenko for assistance at the AFM studies. The work was partially supported by Lithuanian State Science and Education Foundation (project C-03046).

References

[1] I. Šimkienė, Porous dielectric and semiconductor films in nanotechnology, Lithuanian J. Phys. **43**, 319–334 (2003).

[2] P. Moriarty, Nanostructured materials, Rep. Progr. Phys. **64**, 297–381 (2001).

[3] N.K. Raman, M.T. Anderson, and C.J. Brinker, Template-based approaches to the preparation of amorphous, nanoporous silicas, Chem. Mater. **8**, 1682–1701 (1996).

[4] C.J. Brinker and G.W. Scherer, *Sol–Gel Science, The Physics and Chemistry of Sol–Gel Processing* (Academic Press, San Diego, 1990).

[5] G. Wu, J. Wang, J. Shen, T. Yang, Q. Zhang, B. Zhou, Z. Deng, B. Fan, D. Zhou, and F. Zhang, A new method to control nano-porous structure of sol–gel-derived silica films and their properties, Mater. Res. Bull. **36**, 2127–2139 (2001).

[6] P. Tandon and H. Boek, Experimental and theoretical studies of flame hydrolysis deposition process for making glasses for optical planar devices, J. Non-Cryst. Solids **317**, 275–289 (2003).

[7] S. Das, S. Roy, A. Patra, and P.K. Biswas, Study of refractive index and physical thickness of porous silica films with ageing in hydrated ammonia and air, Mater. Lett. **57**, 2320–2325 (2003).

[8] M. Trau, N. Yao, E. Kim, Y. Xia, G.M. Whitesides, and I.A. Aksay, Microscopic patterning orientated mesoscopic silica through guided growth, Nature **390**, 674–676 (1997).

[9] N.K. Raman, M.T. Anderson, and C.J. Brinker, Template-based approaches to the preparation of amorphous, nanoporous silicas, Chem. Mater. **8**, 1682–1701 (1996).

[10] R.M.A. Azzam and N.M. Bashara, *Ellipsometry and Polarized Light* (North-Holland, Amsterdam, 1977).

[11] G.J. Babonas, L. Leonyuk, V. Maltsev, R. Szymczak, A. Reza, M. Baran, and L. Dapkus, Physical properties of $(M_2Cu_2O_3)_m(CuO_2)_n$ (M = Ca, Sr, Bi) single crystals with Bi-2212 phase on their surface, Acta Phys. Pol. A **100**, 553–563 (2001).

[12] M. Born and E. Wolf, *Principles of Optics* (Pergamon Press, Oxford, 1968).

[13] C.M. Herzinger, B. Johns, W.A. McGaham, J.A. Woollam, and W. Paulson, Ellipsometric determination of optical constants for silicon and thermally grown silicon dioxide via a multi-sample, multi-wavelength, multi-angle investigation, J. Appl. Phys. **83**, 3323–3336 (1998).

[14] `http://www.sopra-sa.com`

[15] G. Wu, J. Wang, J. Shen, T. Yang, Q. Zhang, B. Zhou, Z. Deng, B. Fan, D. Zhou, and F. Zhang, A novel route to control refractive index of sol–gel derived nanoporous silica films used as broadband antireflective coatings, Mater. Sci. Engn. B **78**, 135–139 (2000).

[16] J. Ohta, H. Imai, and H. Hirashima, Direct deposition of silica films using silicon alkoxide solution, J. Non-Cryst. Solids **241**, 91–97 (1998).

[17] S. Bruni, F. Cariati, M. Casu, A. Lai, A. Musinu, G. Piccaluga, and S. Solinas, IR and NMR study of nanoparticle-support interactions in Fe_2O_3–SiO_2 nanocomposite prepared by sol–gel method, Nanostruct. Mater. **11**, 573–586 (1999).

[18] X. Wang, X. Chen, X. Ma, H. Zheng, M. Ji, and Z. Zhang, Low-temperature synthesis of α-Fe_2O_3 nanoparticles with a closed cage structure, Chem. Phys. Lett. **384**, 391–393 (2004).

[19] B. Smarsly, G. Garnweitner, R. Assink, and C.J. Brinker, Preparation and characterization of mesostructured polymer-functionalized sol–gel-derived thin films, Prog. Organic Coatings **47**, 393–400 (2003).

[20] S. Pevzner, O. Regevu, and R. Yerushalmi-Rozen, Thin films of mesoporous silica: Preparation and characterization, Current Opinion in Colloid & Interface Science **4**, 420–427 (2000).

[21] I. Simkiene, J. Sabataityte, J.G. Babonas, A. Reza, R. Szymczak, H. Szymczak, M. Baran, M. Kozlowski, and S. Gierlotka, Sol–gel processed iron-containing silica films on Si, Proc. SPIE (accepted).

[22] I. Šimkienė, M. Baran, G.J. Babonas, R.A. Bendorius, A. Reza, R. Szymczak, P. Aleshkevych, R. Šustavičiūtė, and R. Tamaševičius, Formation of iron-containing clusters in silica of predetermined porosity, Acta Phys. Pol. A (submitted).

[23] Landolt-Börnstein, *Numerical Data and Functional Relationships in Science and Technology*, Vol. 17, ed. K.-H. Hellwege (Springer-Verlag, Berlin, 1982).

[24] N. Ozer and F. Tepehan, Optical and electrochemical characteristics of sol–gel deposited iron oxide films, Sol. Energy Mater. Sol. Cells **56**, 141–152 (1999).

[25] W.F. Fontijn, P.J. van der Zaag, M.A.C. Devillers, V.A.M. Brabers, and R. Metselaar, Optical and magneto-optical polar Kerr spectra of Fe_3O_4 and Mg^{2+}- or Al^{3+}-substituted Fe_3O_4, Phys. Rev. B **56**, 5432–5442 (1997).

PORĖTŲJŲ SiO_2 SLUOKSNIŲ ANT Si SUDARYMAS IR TYRIMAS

R. Šustavičiūtė [a,b], I. Šimkienė [a,b], J. Sabataitytė [a], A. Rėza [a], A. Kindurys [a], R. Tamaševičius [a,c], J. Babonas [a,c]

[a] *Puslaidininkių fizikos institutas, Vilnius, Lietuva*
[b] *Vilniaus universitetas, Vilnius, Lietuva*
[c] *Vilniaus Gedimino technikos universitetas, Vilnius, Lietuva*

Santrauka

Zolio ir gelio bei sukininio padengimo metodu pagaminti ir ištyrinėti įvairūs porėtojo silicio dioksido sluoksniai ant Si padėklų. Panaudojant rastrinį elektroninį ir atominės jėgos mikroskopus, buvo tiriama pagamintų sluoksnių morfologija, o jų optinės savybės buvo nustatomos iš elipsometrinių matavimų. Nagrinėta Si dioksido sluoksnių savybių priklausomybė nuo gaminimo ir atkaitinimo sąlygų. Tankūs vienalyčiai 5–9% vidutinio porėtumo ir 250 nm paviršiaus netolygumo SiO_2 sluoksniai buvo pagaminti iš tetraetoksisilano pagrindu paruoštų tirpalų ant ∅5 cm Si plokštelių. Šių ∼250 nm storio sluoksnių porėtumas, einant nuo paviršiaus į padėklą, keitėsi 7–23% ribose. SiO_2 sluoksnių, atkaitintų 300–600 °C temperatūroje, vidutinis lūžio rodiklis atitinkamai padidėjo iki 1,42–1,46. Padidinto porėtumo Si dioksido sluoksniai buvo pagaminti iš tirpalo, kuriame buvo cetiltrimetilamonio bromidas, veikiantis kaip surfaktantas. Tos serijos bandiniuose atkaitinto SiO_2 sluoksnio porėtumas siekė ∼65%, palyginus su 7–10% porėtumu naujai pagamintuose ir dar neatkaitintuose sluoksniuose. Taip pat buvo pagaminti ir ištirti hibridiniai dariniai, porėtieji Si dioksido sluoksniai su įterptomis Fe ir Fe oksidų dalelėmis. Remiantis spektroskopiniais tyrimais išaiškinta, kad Fe oksidai yra Fe_2O_3, Fe_3O_4 ir FeOOH, o atkaitintuose sluoksniuose padidėja santykinis Fe_3O_4 kiekis.